



Pitch-angle distribution evolution of energetic electrons in the inner radiation belt and slot region during the 2003 Halloween storm

Fuliang Xiao,^{1,2} Qiu-Gang Zong,^{3,4} and Liangxu Chen¹

Received 29 January 2008; revised 31 October 2008; accepted 17 November 2008; published 29 January 2009.

[1] In this study, we report dynamic evolutions of 30–500 keV energetic electrons (in flux and pitch-angle distribution) in the radiation belt region with $1.6 < L < 6.2$. Those evolutions were observed by the IES instrument on board the Polar spacecraft during the Halloween storm period on October 31, 2003 when the radiation belt was strongly distorted. This injection of energetic electrons into the slot region may be associated with the plasmopause movement and Hiss/Chorus enhancement. This flux enhancement is possibly associated with convective transport from the plasma sheet, enhanced radial diffusion and local wave-particle interaction acceleration. By adopting a fitting parameter of loss time τ_L we solved the bounce-averaged pitch angle diffusion equation driven by field-aligned whistler-mode waves (including chorus and hiss). We show that pitch-angle scattering can account for the pitch-angle distribution evolution in 30–500 keV electrons in the innermost radiation belt near $L = 1.7$ (as observed by Polar satellite) and the slot region $2 < L < 3$. In particular, simulated results indicate that the loss-cone region is almost empty, and outside the loss-cone region both flux and anisotropy of energetic electrons are reduced with the gyroresonant time. The obtained time scale for the pitch-angle distribution evolution is found to be approximately tens of hours, consistent with observation.

Citation: Xiao, F., Q.-G. Zong, and L. Chen (2009), Pitch-angle distribution evolution of energetic electrons in the inner radiation belt and slot region during the 2003 Halloween storm, *J. Geophys. Res.*, *114*, A01215, doi:10.1029/2008JA013068.

1. Introduction

[2] The radiation belts of the Earth are distributed in two distinct regions, where energetic charged particles are trapped by the Earth's magnetic field. The inner belt is relatively stable and usually exhibits only minor variability to solar wind fluctuations. In contrast, the outer belt is highly variable particularly during geomagnetic storms or other disturbances, with flux changes of energetic electrons exceeding several orders of magnitude over periods from hours to days [Li *et al.*, 1997, 2005b; Reeves *et al.*, 1998, 2003; Zong *et al.*, 2007], leading to potential hazard to spacecrafts in the magnetosphere [Baker, 2002]. This dramatic enhancement in the flux of energetic electrons can be attributed to stochastic acceleration driven by cyclotron wave-particle interaction [Horne and Thorne, 1998; Summers *et al.*, 1998, 2002, 2004, 2007a, 2007b; Roth *et al.*, 1999; Summers and Ma, 2000; Meredith *et al.*, 2002a, 2002b, 2003a; Horne *et al.*, 2003a, 2005a; Li *et al.*, 2005a; Iles *et al.*, 2006; Xiao *et al.*, 2006a, 2007a], together

with inward radial diffusion through drift resonance with enhanced ULF waves [Li *et al.*, 1999, 2001; Brautigam and Albert, 2000; Li and Temerin, 2001; Li, 2004; Barker *et al.*, 2005; Sarris *et al.*, 2006]. Electromagnetic waves (including whistler-mode and EMIC waves) can also produce pitch-angle scattering of electrons [Abel and Thorne, 1998a, 1998b; Summers *et al.*, 1998; Horne *et al.*, 2003b; Summers and Thorne, 2003], resulting in precipitation loss into the atmosphere and ozone destruction by change of atmospheric chemistry [Thorne, 1977; Callis *et al.*, 1998].

[3] During the 2003 Halloween storm, the radiation belts were strongly distorted [Baker *et al.*, 2004; Green and Kivelson, 2004; Li *et al.*, 2006]. A large number of energetic (hundreds of keV or above) electrons were injected into the slot region [Baker *et al.*, 2004]. Particularly, the pitch angle distribution evolution of energetic electrons was observed by the IES instrument on Polar spacecraft. Both radial diffusion and local wave acceleration can contribute to energetic electron flux enhancements in the slot region [Loto'aniu *et al.*, 2006; Thorne *et al.*, 2007]. Although wave-induced electron precipitation is a well known effect, simultaneous measurements of wave bursts and particle precipitation are scarce [Skoug *et al.*, 1996]. One such attempt was made by Walt *et al.* [2002]. In their study, the particle data obtained by the Source/Loss Cone Particle Spectrometer (SEPS) on board the Polar satellite [Blake *et al.*, 1995] provide very interesting results, suggesting that trapped electrons were scattered into the loss cone by electromagnetic waves. Simultaneous observations of electron energy spectra and electron pitch angle distribution with wave characteristics and their time evolution will allow

¹School of Physics and Electronic Sciences, Changsha University of Science and Technology, Changsha, China.

²State Key Laboratory of Space Weather, Chinese Academy of Sciences, Beijing, China.

³School of Earth and Space Sciences, Peking University, Beijing, China.

⁴Center for Atmospheric Research, University of Massachusetts, Lowell, Massachusetts, USA.

Polar IES

Oct. 31, 2003
1700-1726UT

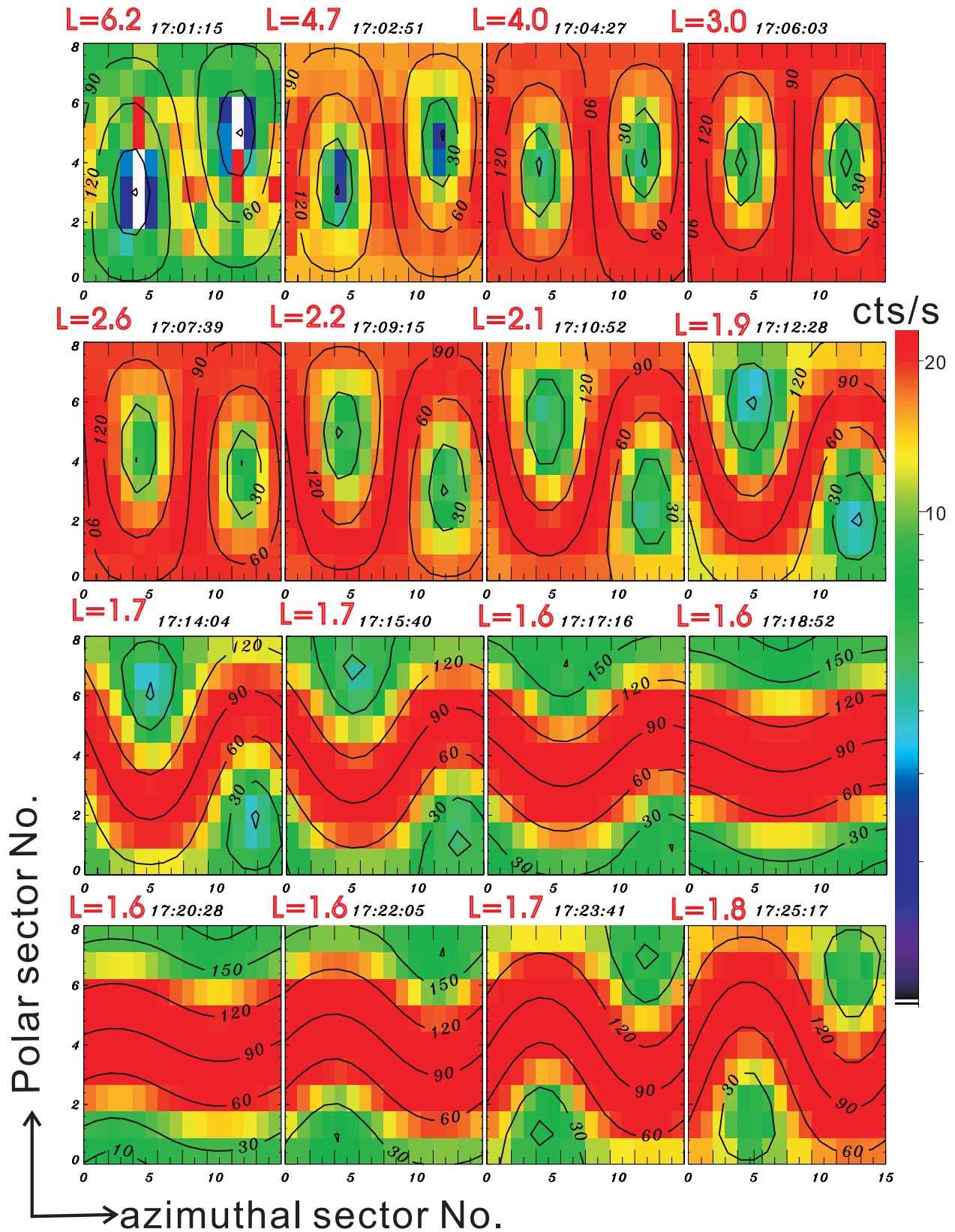


Figure 1

us to assess the efficiency of electrons with different energy interacting with waves. In this study, we report dynamic evolutions of 30–500 keV energetic electrons observed by the IES instrument on board the Polar spacecraft in the radiation belts $1.6 < L < 6.2$ during the Halloween storm period from 29 October to 4 November 2003. We concentrate here on processes responsible for pitch angle distribution evolution of energetic electrons in order to understand transient particle precipitation from the magnetosphere.

2. Observation and Analysis

2.1. Observation

[4] During the 2003 Halloween storm period, the IES instrument on Polar spacecraft collected very valuable data that can be used to study wave-particle interaction in detail. The 3-dimensional energetic electron data from Polar (more than 10 years) satellites are routinely processed and archived. The pitch angle distribution evolution of energetic electrons at a 96-sec resolution is shown in Figure 1. The Polar spacecraft was traveling from GSM (0.2, -0.7 , 1.4) R_E to (1.3, -1.2 , -0.4) R_E . Clearly, a sudden particle intensification (or acceleration) happened at around 17:02:51. A field configuration was also observed by POLAR MFE where the field fluctuation ΔB_0 varied in a range with approximately less than 2% of the ambient magnetic field strength B_0 (<http://www-ssc.igpp.ucla.edu/cgi-bin/polar-master.full>). In general, drift-shell splitting can produce butterfly distributions on the nightside because of distortions from a dipolar configuration [Selesnick and Blake, 2002; Gannon et al., 2007]. Since the dipolar field distortion in that region is found to be very small in the time period of interest, the drift shell splitting effect is not significant. Those energetic electrons peaked at pitch angle 90° well before and after the intensifications, implying a mechanism (possibly associated with inward radial diffusion and/or wave-particle interaction) that energizes particles preferentially at pitch angle 90° [e.g. Baker et al., 2004]. Four selected line plots of electron fluxes versus pitch angles at different L -shells are given in Figure 2, in which electron distributions inside the loss cone are clearly shown. Electron flux versus pitch angle obtained from different energy channels is shown in Figure 3. Furthermore, Figure 4 shows in detail that a large amount of highly energetic (2–6 MeV) electrons were injected into the slot region $2 < L < 3$ on 31 October and remained there for tens of days. Basically, there are three possible mechanisms responsible for the flux enhancement of energetic electrons during geomagnetic storms [e.g., Thorne et al., 2007]: convective transport from the plasma sheet, inward radial diffusion associated with ULF wave and local acceleration through gyroresonant wave-particle interaction. In the following we shall analyze those different mechanisms occurring in the magnetosphere and present brief interpretations for the observational data above.

2.2. Analysis

[5] During geomagnetic storms, the enhanced convection electric field can drive plasma sheet particles into the inner magnetosphere, leading to the formation of the storm-time ring current [Daglis et al., 1999; Jordanova et al., 2003], a redistribution of thermal plasma in the inner magnetosphere [Goldstein et al., 2005], and particularly a kinetic energy gain of particles due to conservation of the first adiabatic invariant and total energy. Recent computer simulation [Liu et al., 2003] has shown that this convective injection can adequately explain the observed injection of ring current electrons at energies below 150 keV during the October 1990 storm. However, Thorne et al. [2007] proposed that injection of higher energy electrons (above 150 keV) into the region $3 \leq L \leq 5$ should be attributed to a different process due to the large gradient drift of higher energy electrons.

[6] ULF wave activity can be greatly enhanced during magnetic storms [Mathie and Mann, 2000; Zong et al., 2007], yielding inward radial diffusion and an associated increase in energetic electron flux [Kivelson and Russell, 1995; Elkington et al., 2003; Shprits et al., 2005; Sarris et al., 2006]. Brautigam and Albert [2000] have solved the standard radial diffusion equation [Schulz and Lanzerotti, 1974] and shown that radial diffusion process can account for the significant variation in the <1 MeV electron flux during the October 9, 1990 geomagnetic storm. Shprits and Thorne [2004] have further demonstrated that enhanced ULF wave activity and strong gradients in phase space density inside $L \sim 4$ could possibly enhance the transport of energetic outer zone electrons into the lower- L region. Loto'aniu et al. [2006] have calculated the rate of radial diffusion by intense ULF waves at the onset of the 29 October 2003 Halloween storm and shown that drift resonant acceleration can occur in the slot region near $L = 2$ over a timescale of 24 hours. However, the significant electron acceleration up to \sim MeV during the 2003 Halloween storm should be attributed to chorus-particle interaction [Baker et al., 2004; Horne et al., 2005b; Shprits et al., 2006a]. Therefore, convective transport and particularly enhanced inward radial diffusion can adequately account for the enhancement in fluxes of 30–500 keV (Figure 1) during the 2003 Halloween storm. However, cyclotron wave-particle interaction should be responsible for the pitch-angle distribution evolution of energetic (30–500 keV) electrons in this storm both in the slot region $2 < L < 3$ (Figure 2) and the inner radiation belt (Figure 3). This will be presented in detail in the following section.

3. Simulation Model

[7] Energetic electrons in the inner magnetosphere may be randomly scattered by various electromagnetic waves including EMIC and whistler-mode waves [Summers and Thorne, 2003; Li et al., 2007], particularly during geomag-

Figure 1. Series of three dimensional electron (30–500 keV) angle-angle distributions (in counts/s) in the perigee region observed by Polar IES during the 2003 Halloween storm time period. The ordinate (X) axis is sectorized data perpendicular to the s/c spin axis, and the abscissa (Y) axis is nine detectors looking directions along the spin axis. The color coding shows the particle flux. The contours indicate the angle between the magnetic field and viewing direction. Lower fluxes along the magnetic field indicate a loss cone. The L -value of the satellite is given above each frame.

Polar IES

31 Oct 2003 17:21--17:47UT

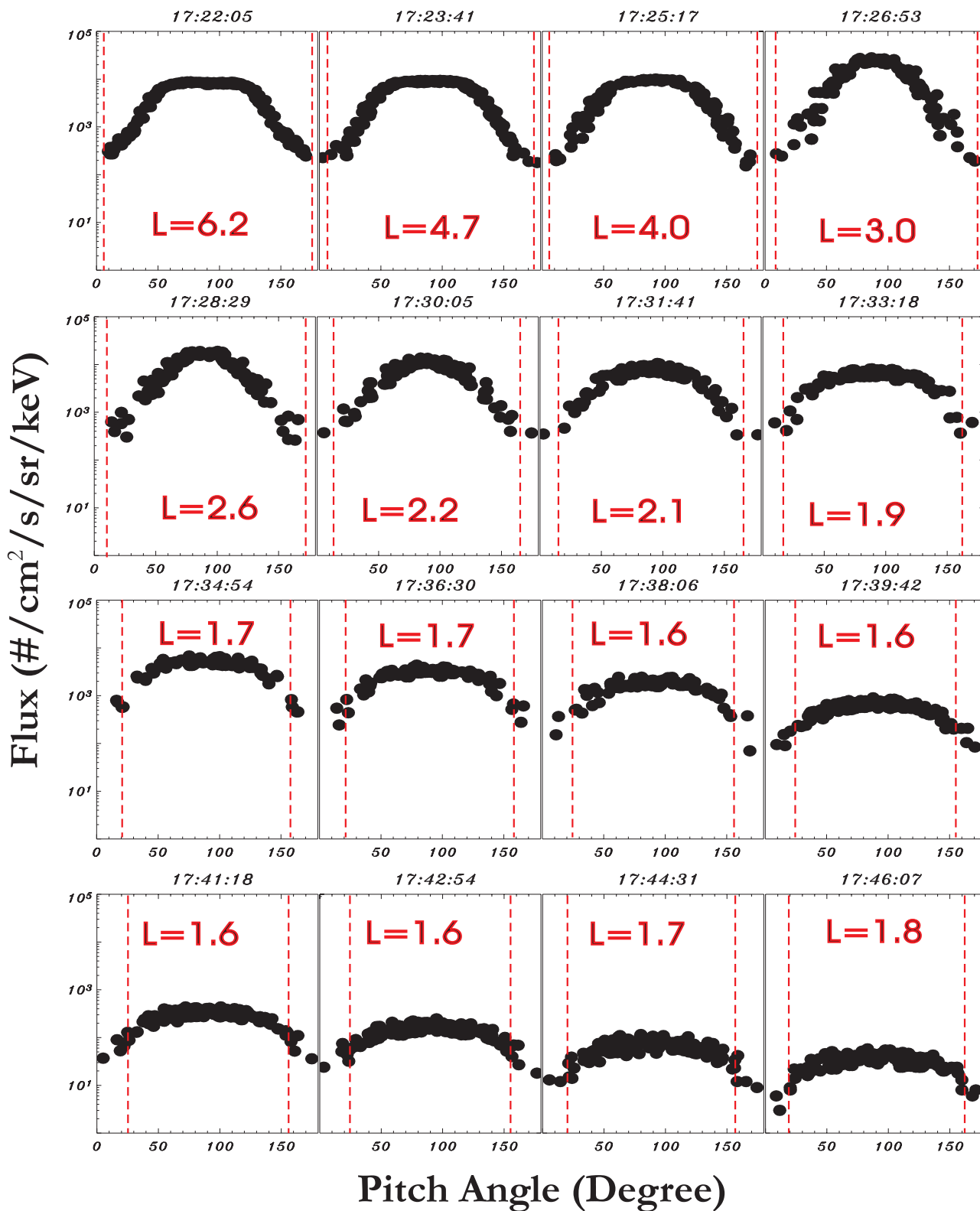


Figure 2. Pitch angle distributions of the differential flux through the inner magnetosphere trapped region from 1723 UT to 1744 UT on 31 October 2003 measured by the Polar IES from the angle-angle plots shown in Figure 1. The dashed lines mark the loss cone. The pitch angle distribution evolution at different L -shells can clearly be identified.

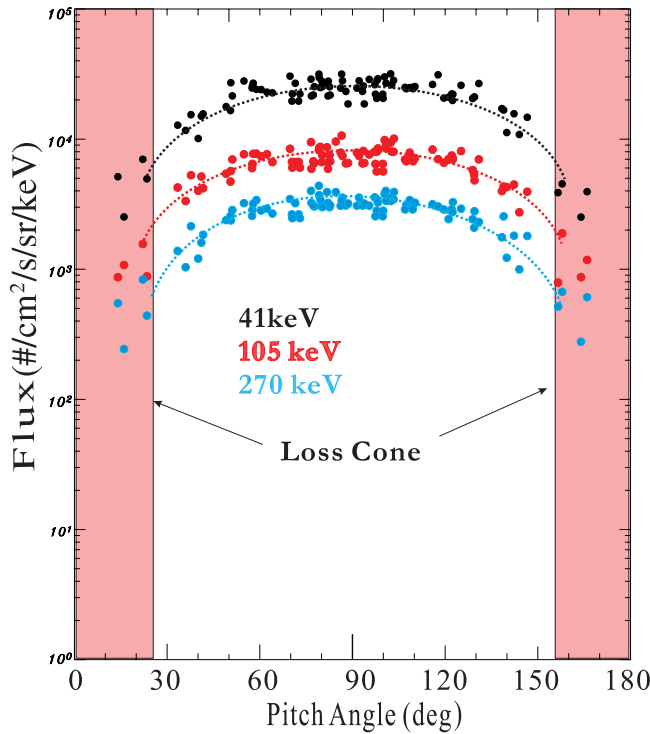


Figure 3. Pitch angle distributions of the differential flux at three electron energy bands in the inner magnetosphere trapped region at 1736 UT on 31 October 2003 measured by the Polar IES. The shaded area marks the loss cone.

netic storms since those waves can be greatly excited [e.g., Xiao *et al.*, 2007b]. Enhanced inward convection provides a seed population of 10 keV to ~ 100 keV electrons throughout the region exterior to the storm-time plasmopause. Conservation of the first two adiabatic invariants leads to anisotropic electron distributions with $T_{\perp} > T_{\parallel}$ (where T_{\perp} and T_{\parallel} denote temperatures perpendicular and parallel to the ambient magnetic field, respectively) during inward transport. Anisotropic electron distributions can yield the excitation of whistler-mode chorus waves at frequencies below the electron gyrofrequency [Horne *et al.*, 2003b; Xiao *et al.*, 2006b], especially in the relativistic case [Xiao *et al.*, 1998, 2006c]. Wave growth is basically associated with pitch-angle scattering to smaller pitch-angles and a net loss of electron energy [e.g., Kennel and Petschek, 1966; Gendrin, 1981]; while wave damping is associated with pitch-angle scattering to larger pitch-angles and electron energization [e.g. Thorne and Horne, 1996]. Statistically, a particle has an equal chance to increase or to decrease its pitch angle after a collision. However, near the loss cone more particles reduce their pitch angles than those increasing their pitch angles because there are fewer particles within the loss cone due to precipitation and lose into the Earth's atmosphere. This process of reduction in the pitch angle can be extended to the whole population. A stably trapped pitch angle distribution would have a peak at 90 degree and decrease monotonically to the field aligned direction [Kennel and Petschek, 1966; Lyons and Thorne, 1972; Schulz and Lanzerotti, 1974; Davidson and Walt, 1977]. This process is the so-called particle pitch angle diffusion.

[8] Plasmaspheric hiss is a broadband ELF whistler mode emission in the frequency range from ~ 100 Hz to several kHz. Hiss occurs in a broad range of the plasmasphere with the innermost boundary of the plasmasphere located at $2 < L < 3$ during storms and around $L = 5$ or 6 during quiet periods. Hiss can also be present outside the plasmasphere, e.g., in detached plasma regions [Parrot and Lefeuvre, 1986]. Plasmaspheric hiss can be greatly enhanced during storms or substorms [Smith *et al.*, 1974; Thorne *et al.*, 1974] with typical broadband amplitudes from 10 pT during quiet periods [Tsurutani *et al.*, 1975] to 100 pT during the recovery phase of storms [Smith *et al.*, 1974].

[9] Whistler-mode chorus emissions are observed outside the plasmopause over a broad range of local times (2200-1300 MLT) with typical frequencies in the range $0.05\text{--}0.8 |\Omega_e|$, where $|\Omega_e|$ is the electron gyrofrequency [Tsurutani and Smith, 1974, 1977; Koons and Roeder, 1990; Meredith *et al.*, 2001; Santolik *et al.*, 2003, 2004]. Typical chorus amplitudes are found to be 1–100 pT [Burtis and Helliwell, 1975; Meredith *et al.*, 2003b], and during intense geomagnetic activity amplitudes even approach 1 nT [Parrot and Gaye, 1994]. Chorus emissions are predominantly substorm dependent, and all chorus emissions intensify when substorm activity is enhanced [Meredith *et al.*, 2001]. In general, although chorus is not often observed throughout the inner magnetosphere, only hiss, lightning and transmitter signals are present [e.g., Green *et al.*, 2005; Meredith *et al.*, 2007]. Smith *et al.* [2004] showed that during larger storms whistler-mode waves were greatly intensified at higher frequencies in the chorus band (e.g., 3 kHz), suggesting that chorus source region is located on lower L -shells than for weaker storms. During the Halloween storms, since the radiation belt was strongly compressed and the plasmopause (which is favorable to chorus generation) moves inwards dramatically even approaching as close as $1.5R_E$ at some longitudes [Baker *et al.*, 2004], we expect whistler-mode chorus waves to be present in the inner magnetosphere. Unfortunately, there are little direct wave observations in the new radiation belt inside $L = 2$ during this event. Figure 5 presents Radio Plasma Imager (RPI) spectrogram with wave frequency lying in the typical whistler-mode chorus frequency range around locations $L = 1.7\text{--}2$ in the storm-time period of interest, consistent with the existing theory that chorus is generally present beyond the plasmopause. Strong wave activities (identified as whistler-mode chorus) are indeed found to occur during UT 2003.10.30.22–2003.10.31.01, giving a basic support for our results below. In addition, whistler mode chorus waves which were excited at some other locations can be guided along the magnetic field [e.g., Horne *et al.*, 2005b], in the modeling described below, we therefore assume that the typical measurements of chorus and hiss power spectral intensity (as mentioned above) are representative of emissions over this storm-period of pitch-angle diffusion of electrons.

[10] Shprits *et al.* [2006b] found that under an assumption of the wave energy being distributed over a range of wave normal angles, bounce-averaged pitch angle and energy diffusion coefficients for the case of field-aligned propagation, agree well with exact calculations with the PADIE

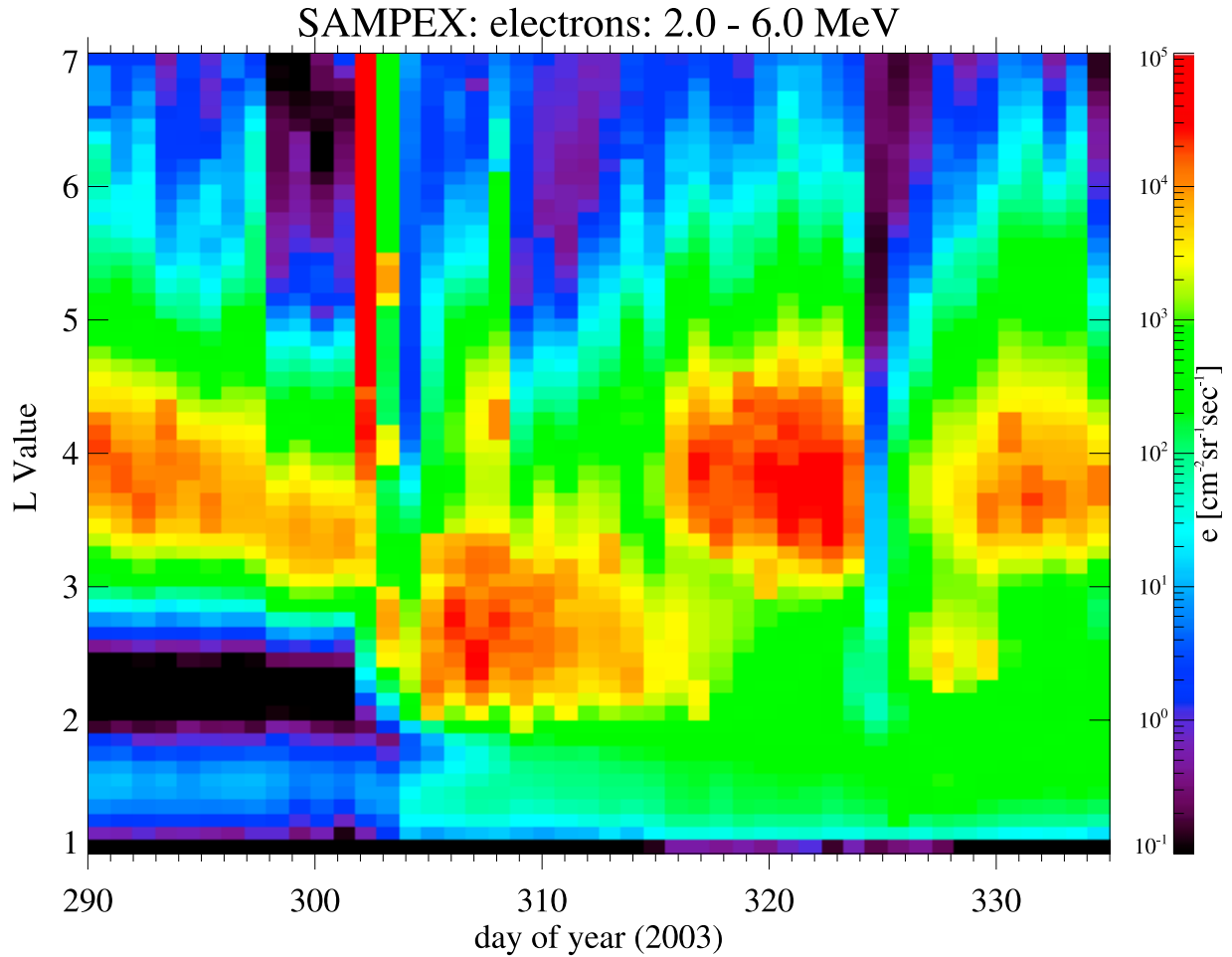


Figure 4. Modified from *Baker et al.* [2004], an injection of a large amount of highly energetic (2–6 MeV) electrons into the slot region occurred on October 31, 2003 and maintained tens of days.

code [Glauert and Horne, 2005]. We therefore adopt the simpler field-aligned scattering model for our simulation.

[11] Temporal evolution of the electron phase space density for a simplified pure bounce-averaged pitch-angle scattering Fokker-Planck equation can be written [Lyons and Williams, 1984]:

$$\frac{\partial f}{\partial t} = \frac{1}{G} \frac{\partial}{\partial \alpha_0} \left(G \hat{D}_{\alpha_0 \alpha_0} \frac{\partial f}{\partial \alpha_0} \right) - \frac{f}{\tau_L} \quad (1)$$

where $G = T_B(\alpha_0) \sin \alpha_0 \cos \alpha_0$ with α_0 being the equatorial pitch angle; $T_B(\alpha_0) \approx 1.30 - 0.56 \sin \alpha_0$ is the normalized bounce period [Lyons et al., 1972], τ_L is the electron loss time determined from a best fitting parameter with observational data inside the loss cone, and set to infinity outside the loss cone. Pitch-angle distribution evolution of energetic electrons can be obtained by a standard correlation between the solution of equation (1) and the differential flux $j = p^2 f$ associated with particle's momentum p [Schulz and Lanzerotti, 1974].

[12] In general, the loss time was assumed to equal the electron quarter bounce time inside the loss cone in previous work [Kennel and Petschek, 1966; Thorne et al., 2005, 2007]. This is an excellent theoretical assumption which is found to be applicable in most cases. However, if the loss-

cone size is relatively large (e.g., at smaller L -shell regions), probably yielding particles to stay a longer time inside the loss-cone without being lost into the atmosphere very rapidly, the loss-cone region is not totally empty particularly near the loss-cone edge (see Figures 2–3). In those cases, the condition of τ_L being one quarter of a bounce period would not be always reasonable since τ_L is fairly small. For instance, at $L \approx 2.5$, for ~ 100 keV electrons, we found $\tau_L \approx 0.03$ s. The loss term associated with $1/\tau_L$ in (1) will dominate and cause the distribution function to decay very rapidly, inconsistent with observation. Therefore, we use τ_L to be a fitting parameter and expect this would be an alternative realistic way to study pitch angle diffusion process particularly inside the loss-cone, at least in the cases of interest.

[13] The bounce-averaged pitch-angle diffusion coefficient occurring in (1) for a dipolar geomagnetic field model is given by:

$$\hat{D}_{\alpha_0 \alpha_0} = \frac{1}{T_B} \int_0^{\lambda_m} D_{\alpha\alpha} \frac{\cos \alpha}{\cos^2 \alpha_0} \cos^7 \lambda d\lambda \quad (2)$$

where λ is the geomagnetic latitude, λ_m is the mirror point latitude, $D_{\alpha\alpha}$, which denotes the overall local pitch-angle diffusion coefficient due to the combined contribution of

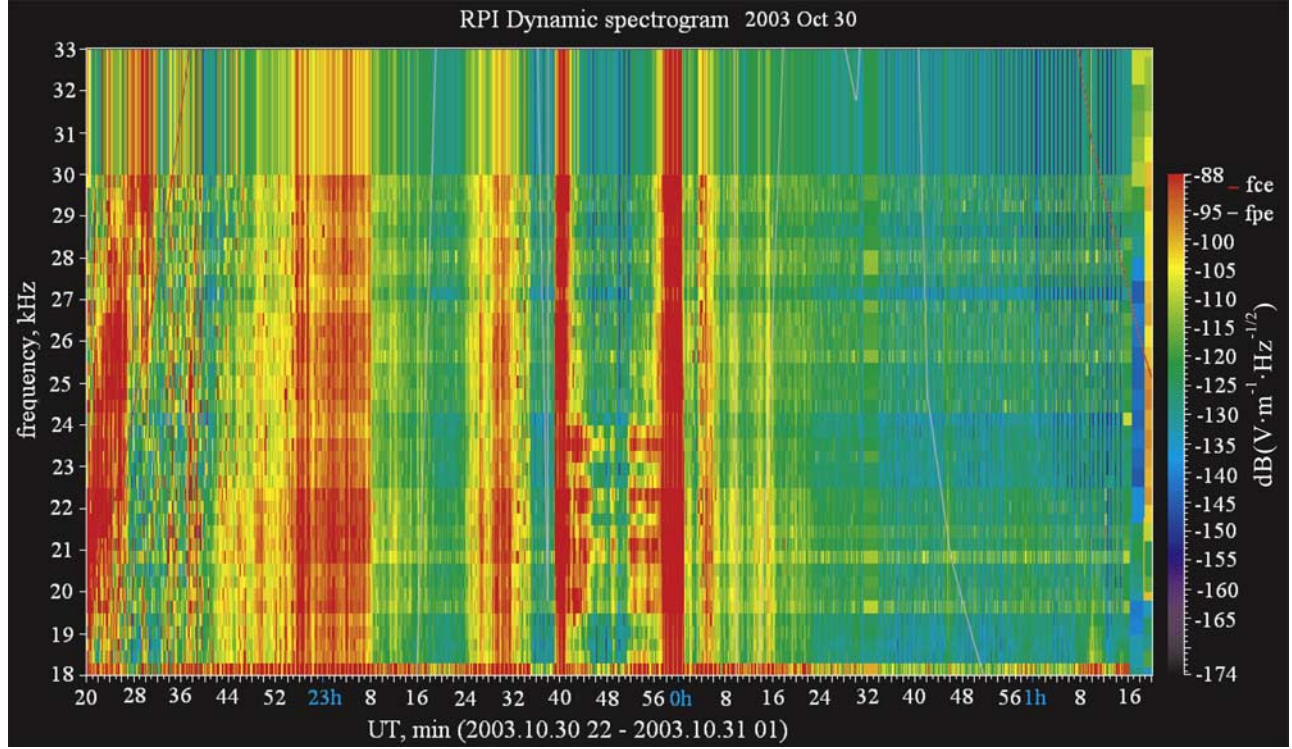


Figure 5. RPI spectrogram with wave frequency lying in the typical whistler-mode chorus frequency range around location $L = 1.7-2$. Strong wave activities (identified as whistler-mode chorus) are found to occur during UT 2003.10.30.22-2003.10.31.01.

chorus and hiss, has been well documented in previous papers [Steinacker and Miller, 1992; Summers, 2005; Summers et al., 2007a]:

$$D_{\alpha\alpha} = \frac{|\Omega_e|^2}{p_s^2} \left(I_0 \frac{p_s^2}{\gamma^2} - 2I_1 \frac{p_s}{\gamma} \cos \alpha + I_2 \cos^2 \alpha \right) \quad (3)$$

and

$$I_n = \pi \sum_{k_{sr}} \frac{B_\omega^2}{B_0^2} \left(\frac{\omega_s}{k_{sr}} \right)^n \left| 1 - \cos \alpha \frac{p_s}{\gamma} \frac{dk_s}{d\omega_s} \right|_{k_s=k_{sr}}^{-1} \quad (4)$$

where $n = 0, 1, 2$; α is the local pitch-angle, $\gamma = (1 + p_s^2)^{1/2}$ is the Lorentz factor with $p_s = p/mc$ being the scaled momentum of electrons, m and c stand for the rest mass of particles and the speed of the light; $|\Omega_e|$ and B_0 represent the local gyrofrequency and the local ambient magnetic field strength; ω_s and k_s are the scaled wave frequency ($\omega_s = \omega/|\Omega_e|$) and wave number ($k_s = ck/|\Omega_e|$), k_{sr} denotes a root of the field-aligned propagated gyroresonant condition in scaled variables: $\gamma \omega_s - k_s p_s \cos \alpha = 1$. The term $dk_s/d\omega_s$ can be evaluated from the standard dispersion relation of field-aligned propagated whistler-mode waves in scaled variables [e.g., Stix, 1992]:

$$k_s^2 = \omega_s^2 - \frac{\rho \omega_s}{\omega_s - 1} \quad (5)$$

[14] Here $\rho = \omega_{pe}^2/|\Omega_e|^2$, and ω_{pe} is the plasma frequency. In the following, we shall assume that the power spectral

density of the wave magnetic field B_ω^2 (in unit of $\text{nT}^2 \text{Hz}^{-1}$) is distributed over a Gaussian frequency distribution with

$$B_\omega^2 = \begin{cases} A^2 \exp[-(\omega - \omega_m)^2/\delta\omega^2] & \text{for } \omega_{lc} \leq \omega \leq \omega_{uc} \\ 0 & \text{otherwise.} \end{cases} \quad (6)$$

where ω_m and $\delta\omega$ are the frequency of maximum wave power and bandwidth, respectively (in rads s^{-1}), and

$$A^2 = \frac{B_t^2}{\delta\omega} \frac{2}{\sqrt{\pi}} \left[\text{erf} \left(\frac{\omega_{uc} - \omega_m}{\delta\omega} \right) + \text{erf} \left(\frac{\omega_m - \omega_{lc}}{\delta\omega} \right) \right]^{-1} \quad (7)$$

[15] Here B_t is the total wave magnitude in unit of nT. The boundary condition are taken $f = 0$ at $\alpha_0 = 0$ and $\partial f/\partial \alpha_0 = 0$ at $\alpha_0 = 90$. The initial condition is chosen:

$$f(\alpha_0, t = 0) = f_0 \sin^q \alpha_0, \quad \text{or,} \quad j(\alpha_0, t = 0) = j_0 \sin^q \alpha_0 \quad (8)$$

where f_0 (or j_0) and q are the best fitting parameters with observational data.

[16] In the following, we shall calculate overall diffusion coefficients $D_{\alpha_0\alpha_0}$ and $\hat{D}_{\alpha_0\alpha_0}$ due to chorus and hiss respectively, and present simulation results for both the inner radiation belt (particularly $L = 1.7$) and the slot region $2 < L < 3$.

4. Results for the Inner Radiation Belt

[17] Evaluation of the pitch-angle diffusion equation (1) requires knowledge of wave data and the plasma density model. The plasma density is assumed to be $N_b = 1390 (3/L)^{4.83}$

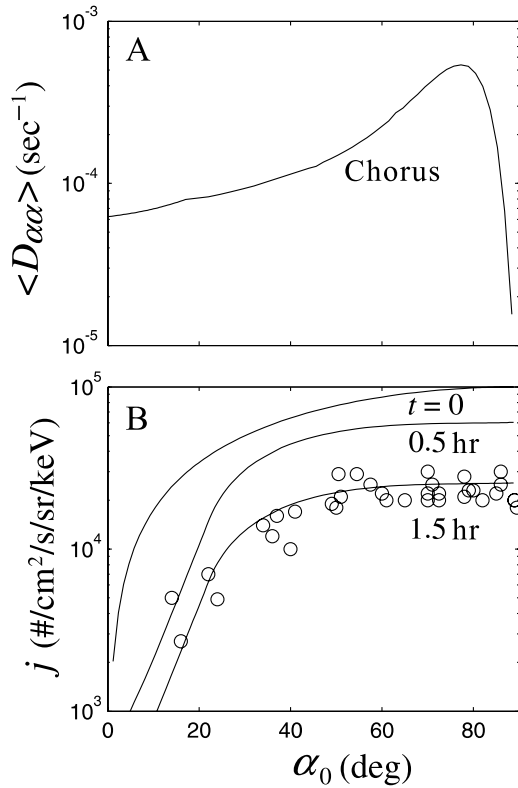


Figure 6. (top) The bounce-averaged diffusion coefficient for chorus at $E_k = 41$ keV. (bottom) Simulation of the flux evolution due to pitch-angle diffusion by chorus emission at $L = 1.7$ with fitting parameters: $q = 1$ and $\tau_L = 100$ s. The discrete circle symbols represent the observational data, and the solid line corresponds to the differential flux obtained by solutions of equation (1) and $j = p^2 f$. Also shown are the indicated respective decay times.

cm^{-3} and remain constant with latitude based on previous work [Sheeley *et al.*, 2001; Summers *et al.*, 2007b; Thorne *et al.*, 2007]. The realistic parameters for stormtime properties of equatorial whistler waves [Meredith *et al.*, 2003b; Horne *et al.*, 2005b; Meredith *et al.*, 2007] are chosen as follows. For chorus: $\lambda_m = 30^\circ$, $B_t = 100$ [pT], $\omega_{lc} = 0.1|\Omega_e|$, $\omega_{uc} = 0.8|\Omega_e|$, $\delta\omega = (\omega_{uc} - \omega_{lc})/4$, $\omega_m = (\omega_{uc} + \omega_{lc})/2$; and for hiss: $\lambda_m = 30^\circ$, $B_t = 100$ [pT], $\delta\omega = (\omega_{uc} - \omega_{lc})/4$, $\omega_m = (\omega_{uc} + \omega_{lc})/2$, $\omega_{lc}/2\pi = 0.1$ kHz, $\omega_{uc}/2\pi = 2.5$ kHz. It should be noted that by using the Maxwell's induction equation and Gaussian frequency distribution (6), the wave amplitude $B_t = 100$ [pT] is found to be comparable to the observed chorus wave intensity dB ($\text{V m}^{-1} \text{Hz}^{-1/2}$) in Figure 5.

[18] In order to obtain exponential decay of the observed electron distribution function (or the differential flux), and correspondingly the precipitation lifetime due to pitch-angle scattering into the atmosphere, knowledge of the initial flux j_0 (in unit of $(\text{cm}^2 \text{s sr keV})^{-1}$) is needed. Based on the standard AE 5 model, we choose $j_0 = 10^5$ at $E_k = 41$ keV, 8.5×10^4 at 105 keV, and 2.5×10^4 at 270 keV.

[19] In Figures 6–8, we present a realistic simulation (top panels) of the flux evolution at three typical energies $E_k = 41, 105$ and 270 keV with the observation (Figure 3), together

with the corresponding bounce-averaged pitch-angle diffusion coefficient at each energy (bottom panels). The diffusion coefficient for hiss is found to occur only at energy of 270 keV and locates below the loss-cone pitch-angle $\alpha_L \approx 21.6^\circ$, with a peak around $\alpha_0 = 0^\circ$ (see Figure 8), indicating that plasmaspheric hiss has contribution to pitch-angle diffusion only at energy of 270 keV but no contribution at energy of 41 or 105 keV (see Figures 6–7). This result is consistent with previous work that hiss is primarily responsible for pitch-angle scattering of high energetic particles [e.g., Lyons *et al.*, 1972; Summers *et al.*, 2007b]. The diffusion coefficient for chorus is found to be present at those three energies, basically increases with α_0 and reach a maximum above $\alpha_0 = 75^\circ$, implying that chorus can be responsible for pitch-angle scattering at both the loss-cone and particularly large pitch-angles. In bottom panels, the discrete circle symbols represent observational data and the solid lines correspond to fluxes by the subsequent conversion from solutions of equation (1) to the differential flux $j = p^2 f$. The simulation gives an adequate fit to the observed data in each case that the loss-cone region is almost empty, and outside the loss-cone region both flux and anisotropy of energetic electrons are reduced with the gyroresonant time. The best fitting parameters q and particularly τ_L are obtained: $q = 1$ and $\tau_L = 100$ s for 41 keV; $q = 1$ and $\tau_L = 300$ s for 105 keV; and $q = 0.5$ and $\tau_L = 1000$ s for 270 keV, respectively. The parameter q , which describes the steepness of the flux peak around pitch angle 90°

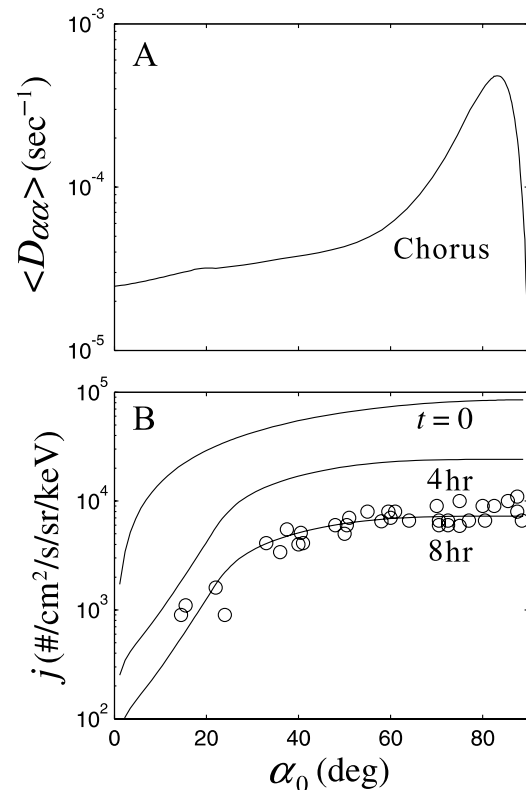


Figure 7. Same as Figure 6 except for $E_k = 105$ keV, and fitting parameters: $q = 1$ and $\tau_L = 300$ s. Also shown are the indicated respective decay times.

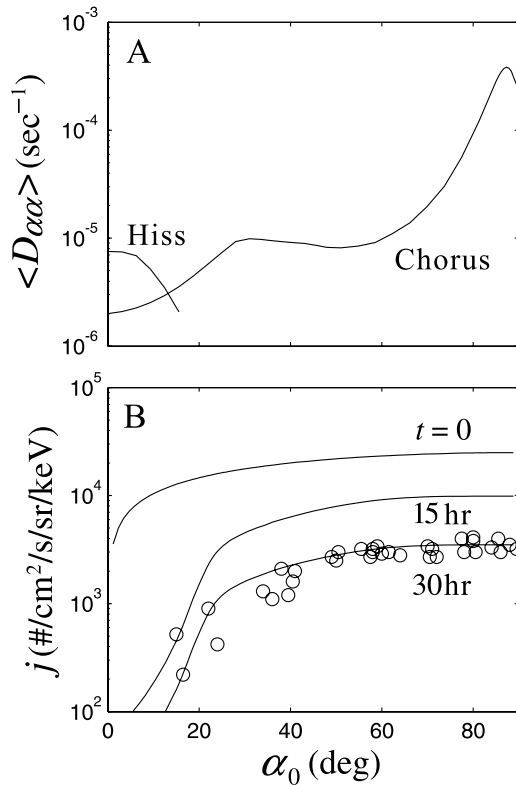


Figure 8. Same as Figure 6 except for $E_k = 270$ keV and the combined contribution of chorus and hiss, and fitting parameters: $q = 0.5$ and $\tau_L = 1000$ s. Also shown are the indicated respective decay times.

associated with inward radial diffusion, basically depends on the L -shell, geomagnetic activities and particle energies [Gannon *et al.*, 2007]. The loss time τ_L is found to be quite different from the electron quarter bounce time, suggesting that perhaps it is more realistic to use the fitting method in some cases. Exponential decay times of the differential flux from initial values to observational data are found to be approximately: 1.5 hours for 41 keV, 8 hours for 105 keV, and 30 hours for 270 keV, consistent with previous studies [e.g., Lyons *et al.*, 1972; Meredith *et al.*, 2007].

5. Results for the Slot Region

[20] Since the plasmopause was strongly compressed and lasted for several days inside $L = 2$ during the Halloween storm, we assume that the plasma density is taken $N_b = 1390(3/L)^{4.83} \text{ cm}^{-3}$ in the region below $L \sim 2.2$ and $N_b = 124(3/L)^4 \text{ cm}^{-3}$ in the region above $L \sim 2.2$ [Sheeley *et al.*, 2001; Summers *et al.*, 2007b], and remain constant with latitude [Thorne *et al.*, 2007]. Similarly, based on the previous work mentioned above, we choose the following parameters for stormtime properties of equatorial whistler waves as variable as possible to incorporate the contribution of both chorus and hiss. At $L = 2.2$ and 2.1 , for chorus: $\lambda_m = 30^\circ$, $B_t = 100$ [pT], $\omega_{lc} = 0.1|\Omega_e|$, $\omega_{uc} = 0.8|\Omega_e|$, $\delta\omega = (\omega_{uc} - \omega_{lc})/4$, $\omega_m = (\omega_{uc} + \omega_{lc})/2$; for hiss: $\lambda_m = 30^\circ$, $B_t = 100$ [pT], $\delta\omega = (\omega_{uc} - \omega_{lc})/4$, $\omega_m = (\omega_{uc} + \omega_{lc})/2$, $\omega_{lc} = 0.001|\Omega_{eq}|$, $\omega_{uc} =$

$0.03|\Omega_e|$. At $L = 3$ and 2.6 , for chorus: $\lambda_m = 30^\circ$, $B_t = 100$ [pT], $\omega_{lc} = 0.2|\Omega_e|$, $\omega_{uc} = 0.8|\Omega_{eq}|$, $\delta\omega = (\omega_{uc} - \omega_{lc})/4$, $\omega_m = (\omega_{uc} + \omega_{lc})/2$; for hiss: $\lambda_m = 30^\circ$, $B_t = 100$ [pT], $\delta\omega = (\omega_{uc} - \omega_{lc})/4$, $\omega_m = (\omega_{uc} + \omega_{lc})/2$, $\omega_{lc} = 0.0025|\Omega_e|$, $\omega_{uc} = 0.18|\Omega_e|$.

[21] Figure 2 clearly shows that in the slot region $2 < L < 3$, pitch angle distribution of particles gradually evolves from a high anisotropy (at $L = 3$ and 2.6) into a quasi-anisotropy (at $L = 2.2$ and 2.1), suggesting that pitch-angle scattering resulted from wave-particle interaction will play more and more important role in the formation of pitch angle distribution with the gyroresonant time. Since observational data (Figure 2) present only pitch angle distribution of the integrated flux ranging from energies 30–500 keV at each location, we shall choose the flux of 300 keV to be representative of the integrated flux behavior and obtain the value following an assumption that the flux obeys a typical power-law $j \sim E^{-\kappa}$ with $\kappa = 5$ comparable to those in previous works [e.g., Freeman *et al.*, 1998; Xiao *et al.*, 2008].

[22] In Figure 9, we present simulations of pitch angle distribution (solid lines) at $L = 2.6$ (left panels) and 3.0 (right panels) with observational data (discrete circle symbols), together with corresponding diffusion coefficients, respectively. The diffusion coefficient for hiss can approach pitch angles above $\alpha_0 \approx 60^\circ$, indicating that hiss can contribute more to pitch angle scattering in the slot region. The best fitting parameters: j_0 , q and particularly τ_L are obtained: $j_0 = 3.5 \times 10^4$, $q = 15$, $\tau_L = 0.09$ s for $L = 2.6$; and $j_0 = 5 \times 10^4$, $q = 15$, $\tau_L = 0.1$ s for $L = 3.0$. The loss time τ_L is found to be comparable to the electron quarter bounce time, suggesting that in the case of a relatively small and empty loss-cone, the current fitting method for τ_L is consistent with the theoretical assumption adopted in previous work [e.g., Kennel and Petschek, 1966; Thorne *et al.*, 2005, 2007]. Exponential decay times of differential fluxes are found to be very rapid: 100 s at $L = 2.6$ and 50 s at 3.0 , implying that pitch angle scattering driven by wave-particle interaction occurs only for a short time in these cases, allowing pitch angle distribution to still remain relatively highly anisotropic (see Figure 2).

[23] Similarly, simulated results of pitch angle distribution (solid lines) at $L = 2.1$ (left panels) and 2.2 (right panels) with observation (discrete circle symbols), together with corresponding diffusion coefficients, are respectively shown in Figure 10. The best fitting parameters τ_L are found to be 1500 s in both regions. Exponential decay times of differential fluxes are found to be approximately: 10 hours at location of $L = 2.1$ and 7 hours at 2.1 , indicating that pitch angle scattering has taken place for a relatively long time in two cases, yielding a quasi-isotropic distribution (see Figure 2).

[24] It should be pointed out that energetic electrons usually drift in approximately circular trajectories eastward about the Earth and intersect the spatial zone of chorus and hiss emissions for more than 50% of their orbit [Summers *et al.*, 2007b]. Therefore drift averaging should be incorporated to obtain more realistic loss-rates. Application of drift averaging should increase loss times (depending on the drift averaging percentage), however, this does not change fundamental properties of pitch angle diffusion process. Since

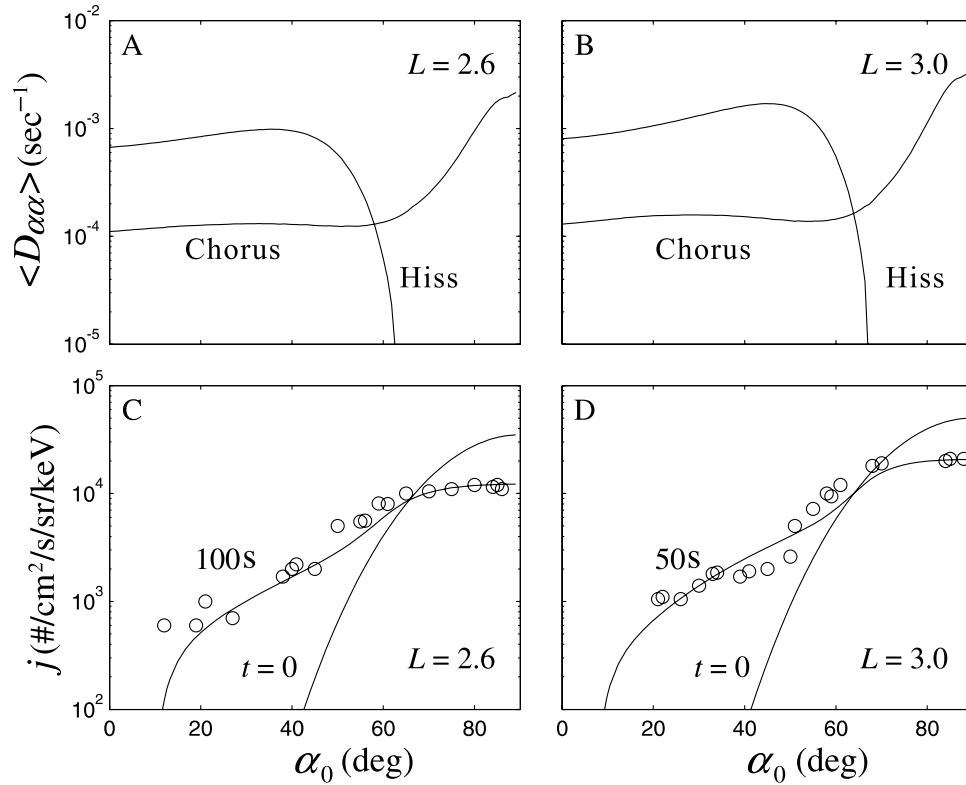


Figure 9. (left) The bounce-averaged diffusion coefficient for $E_k = 300$ keV and the corresponding simulation (solid line) of the flux evolution with the observation (discrete circle symbols) at $L = 2.6$ with fitting parameters: $q = 15$, $j_0 = 3.5 \times 10^4$ and $\tau_L = 0.09$ s. (right) Same but for $L = 3.0$ and fitting parameters: $q = 15$, $j_0 = 5.0 \times 10^4$ and $\tau_L = 0.1$ s. Also shown are the indicated respective decay times.

there is a lack of wave data for guidance, we leave this for future investigation upon wave information available.

6. Summary and Conclusions

[25] In this study, we have reported dynamic evolutions in flux and pitch-angle distribution of energetic electrons (30–500 keV) during the 2003 Halloween storm period when the plasmopause moves inwards dramatically into $L < 2$ [Baker *et al.*, 2004]. We have also shown wave data from Radio Plasma Imager (RPI) spectrogram with frequency lying in the typical chorus frequency range around locations $L = 1.7$ – 2 in the storm-time period of interest, consistent with the previous work that chorus generally occurs beyond the plasmopause. Using the Maxwell’s induction equation, we find the wave amplitude $B_r = 100$ [pT] comparable to the observed chorus wave intensity dB (see Figure 5). The electron flux enhancement in the slot region (normally devoid of energetic electrons) is found to be associated with the plasmopause movement and enhanced Hiss/Chorus wave activity [e.g., Thorne *et al.*, 2007]. We restrict our attention on pitch-angle diffusion process driven by field-aligned whistler-mode waves (including plasmaspheric hiss and chorus) and solved the bounce-averaged pitch angle diffusion equation particularly adopting a fitting parameter of loss time τ_L . We find that pitch-angle diffusion can primarily account for pitch-angle distribution evolution in 30–500 keV electrons in the innermost radiation belt near $L = 1.7$ (as observed by Polar/IES instruments) and the

slot region $2 < L < 3$. The obtained time scale for pitch-angle distribution evolution is found to be a few hours to tens of hours, consistent with observation. The following conclusions can be obtained.

[26] 1. In the inner radiation belt, the plasmaspheric hiss is found to contribute to the energetic electron pitch-angle diffusion at energy of 270 keV with pitch angle near or below the loss-cone region, but does not contribute at energy of 41 or 105 keV, consistent with the previous work that hiss is primarily responsible for pitch-angle scattering of highly energetic particles.

[27] 2. In the slot region, the diffusion coefficient for hiss can approach the pitch angle well above the loss-cone region, even above $\alpha_0 = 60^\circ$ at $L = 2.6$ and 3.0 , suggesting that hiss can contribute more to pitch angle scattering of energetic electrons.

[28] 3. In the inner radiation belt and the slot region, the diffusion coefficient for chorus covers regions from the loss-cone to large pitch-angles and basically increases with pitch angle increasing, implying that chorus can be responsible for pitch-angle scattering near the loss-cone and particularly at large pitch-angles, and primarily produces pitch-angle distribution evolution from a high anisotropy to a quasi-isotropy.

[29] 4. The simulated results successfully mimic observational data that in both regions above, the loss-cone region is almost empty, and above the loss-cone region both flux and anisotropy of energetic electrons are reduced as the gyroresonant time in the course of wave-particle

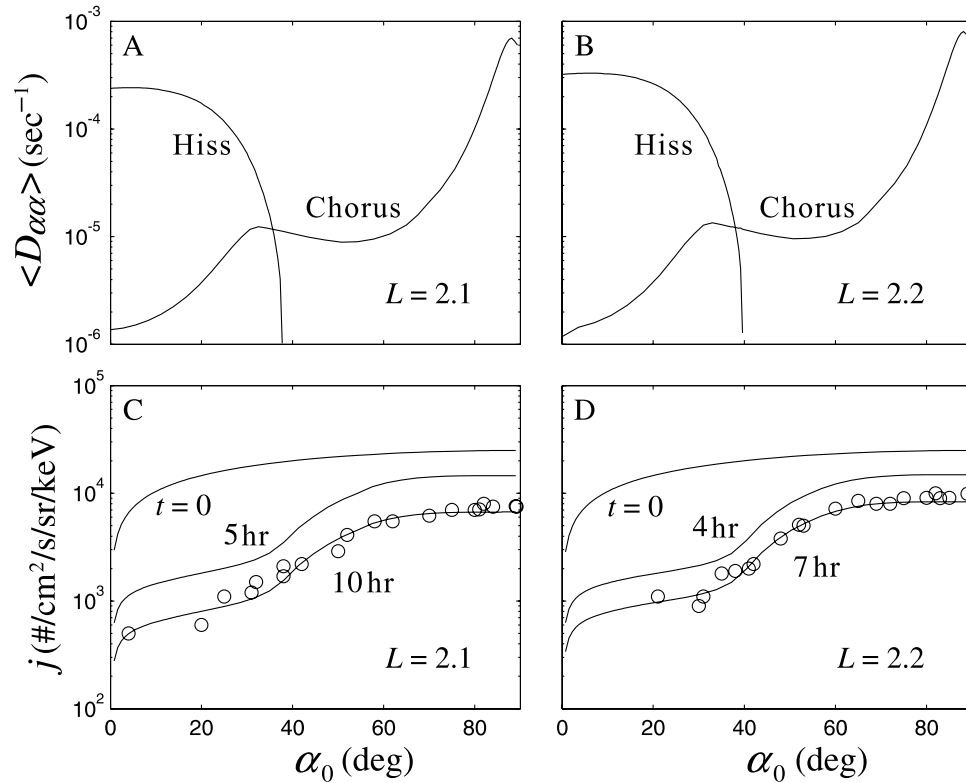


Figure 10. Same as Figure 9 except for $L = 2.1$ (left) and 2.2 (right) and fitting parameters: $q = 0.5$, $j_0 = 2.5 \times 10^4$ and $\tau_L = 1000$ s. Also shown are the indicated respective decay times.

interaction, suggesting that plasmaspheric hiss and chorus can indeed induce the rapid precipitation loss of energetic electrons, and chorus can primarily be responsible for the formation of pitch angle distribution at large pitch angles.

[30] 5. In the case of a small and empty loss-cone, the fitting parameter τ_L is comparable to one quarter of the bounce period which was often used in previous work. However, in the case of a relatively large loss cone (not empty), τ_L is found to be quite different from one quarter of the bounce period, suggesting that perhaps the fitting method is an alternative realistic way to deal with pitch angle scattering in some cases.

[31] The one-dimensional simulation described above suggested that wave-particle scattering provides an effective mechanism to account for pitch angle evolution of energetic (30–500 keV) electron flux in the slot region and the inner radiation belt during the 2003 Halloween storm. In general, dynamics occurring in outer radiation belts are characterized by competition of acceleration and loss of energetic (particularly \sim MeV) electrons due to wave-particle interaction together with radial diffusion. Also energetic electrons usually drift approximately circularly about the Earth and intersect the spatial zone of waves. In order to accurately model this competition, further work is required to incorporate ULF/VLF contribution together by using a 2-D or 3-D simulation associated with pitch angle diffusion, energy diffusion, radial diffusion and bounce-averaging [e.g., *Varotsou et al.*, 2005; *Li et al.*, 2007].

[32] **Acknowledgments.** This work is supported by the National Natural Science Foundation of China grants 40831061, 40774078,

40874076, 40774079; and the Visiting Scholar Foundation of State Key Laboratory of Space Weather, Chinese Academy of Sciences.

[33] Zuyin Pu thanks Jennifer Gannon, S. Gary and three other reviewers for their assistance in evaluating this paper.

References

- Abel, B., and R. M. Thorne (1998a), Electron scattering loss in earth's inner magnetosphere: 1. Dominant physical processes, *J. Geophys. Res.*, *103*, 2385.
- Abel, B., and R. M. Thorne (1998b), Electron scattering loss in earth's inner magnetosphere: 2. Sensitivity to model parameters, *J. Geophys. Res.*, *103*, 2397.
- Baker, D. N. (2002), How to cope with space weather, *Science*, *297*, 1486.
- Baker, D. N., S. G. Kanekal, X. Li, S. P. Monk, J. Goldstein, and J. L. Burch (2004), An extreme distortion of the Van Allen belt arising from the "Halloween" solar storm in 2003, *Nature*, *432*, 878.
- Barker, A. B., X. Li, and R. S. Selesnick (2005), Modeling the radiation belt electrons with radial diffusion driven by the solar wind, *Space Weather*, *3*, S10003, doi:10.1029/2004SW000118.
- Blake, J. B., et al. (1995), Comprehensive energetic particle and pitch angle distribution experiment on POLAR, in *The Global Geospace Mission*, pp. 531–562, Kluwer Acad., Norwell, Mass.
- Brautigam, D. H., and J. M. Albert (2000), Radial diffusion analysis of outer radiation belt electrons during the October 9, 1990, magnetic storm, *J. Geophys. Res.*, *105*, 291.
- Burtis, W. J., and R. A. Helliwell (1975), Magnetospheric chorus: Amplitude and growth rate, *J. Geophys. Res.*, *80*, 3265.
- Callis, L. B., M. Natarajan, D. S. Evans, and J. D. Lambeth (1998), Solar atmospheric coupling by electrons (SOLACE): 1. Effects of the May 12, 1997 solar event on the middle atmosphere, *J. Geophys. Res.*, *103*, 28,405.
- Daglis, I. A., R. M. Thorne, W. Baumjohan, and S. Orsini (1999), The terrestrial ring current: Origin, formation, and decay, *Rev. Geophys.*, *37*, 407.
- Davidson, G., and M. Walt (1977), Loss cone distributions of radiation belt electrons, *J. Geophys. Res.*, *82*, 48.
- Elkington, S. R., M. K. Hudson, and A. A. Chan (2003), Resonant acceleration and diffusion of outer zone electrons in an asymmetric geomagnetic field, *J. Geophys. Res.*, *108*(A3), 1116, doi:10.1029/2001JA009202.

- Freeman, J. W., T. P. O'Brien, A. A. Chan, and R. A. Wolf (1998), Energetic electrons at geostationary orbit during the November 3–4 storm: Spatial/temporal morphology, characterization by a power law and, representation by an artificial neural network, *J. Geophys. Res.*, *103*, 26,251.
- Gannon, J. L., X. Li, and D. Heynderickx (2007), Pitch angle distribution analysis of radiation belt electrons based on Combined Release and Radiation Effects Satellite Medium Electrons A data, *J. Geophys. Res.*, *112*, A05212, doi:10.1029/2005JA011565.
- Gendrin, R. (1981), General relationships between wave amplification and particle diffusion in a magnetoplasma, *Rev. Geophys. Space Phys.*, *19*, 171.
- Glauert, S. A., and R. B. Horne (2005), Calculation of pitch angle and energy diffusion coefficients with the PADIE code, *J. Geophys. Res.*, *110*, A04206, doi:10.1029/2004JA010851.
- Goldstein, J., B. R. Sandel, W. T. Forrester, M. F. Thomsen, and M. R. Hairston (2005), Global plasmaphere evolution 22–23 April 2001, *J. Geophys. Res.*, *110*, A12218, doi:10.1029/2005JA011282.
- Green, J. C., and M. G. Kivelson (2004), Relativistic electrons in the outer radiation belt: Differentiating between acceleration mechanisms, *J. Geophys. Res.*, *109*, A03213, doi:10.1029/2003JA010153.
- Green, J. L., S. Boardsen, L. Garcia, W. W. L. Taylor, S. F. Fung, and B. W. Reinisch (2005), On the origin of whistler mode radiation in the plasmasphere, *J. Geophys. Res.*, *110*, A03201, doi:10.1029/2004JA010495.
- Horne, R. B., and R. M. Thorne (1998), Potential waves for relativistic electron scattering and stochastic acceleration during magnetic storms, *J. Geophys. Res.*, *25*, 3011.
- Horne, R. B., S. A. Glauert, and R. M. Thorne (2003a), Resonant diffusion of radiation belt electrons by whistler mode chorus, *Geophys. Res. Lett.*, *30*(9), 1493, doi:10.1029/2003GL016963.
- Horne, R. B., R. M. Thorne, N. P. Meredith, and R. R. Anderson (2003b), Diffuse auroral electron scattering by electron cyclotron harmonic and whistler mode waves during an isolated substorm, *J. Geophys. Res.*, *108*(A7), 1290, doi:10.1029/2002JA009736.
- Horne, R. B., R. M. Thorne, S. A. Glauert, J. M. Albert, N. P. Meredith, and R. R. Anderson (2005a), Timescale for radiation belt electron acceleration by whistler mode chorus waves, *J. Geophys. Res.*, *110*, A03225, doi:10.1029/2004JA010811.
- Horne, R. B., et al. (2005b), Wave acceleration of electrons in the Van Allen radiation belts, *Nature*, *437*, 227.
- Iles, R. H. A., N. P. Meredith, A. N. Fazakerley, and R. B. Horne (2006), Phase space density analysis of the outer radiation belt energetic electron dynamics, *J. Geophys. Res.*, *111*, A03204, doi:10.1029/2005JA011206.
- Jordanova, V. K., A. Boonsirirath, R. M. Thorne, and Y. Dotan (2003), Ring current asymmetry from global simulations using a high-resolution electric field model, *J. Geophys. Res.*, *108*(A12), 1443, doi:10.1029/2003JA009993.
- Kennel, C. F., and H. E. Petschek (1966), Limit on stably trapped particle fluxes, *J. Geophys. Res.*, *71*, 1.
- Kivelson, M. G., and C. T. Russell (1995), *Introduction to Space Physics*, Cambridge Univ. Press, Cambridge, U.K.
- Koons, H. C., and J. L. Roeder (1990), A survey of equatorial magnetospheric wave activity between 5 and 8 R_E , *Planet. Space Sci.*, *38*, 1335.
- Li, X. (2004), Variations of 0.7–6.0 MeV electrons at geosynchronous orbit as a function of solar wind, *Space Weather*, *2*, S03006, doi:10.1029/2003SW000017.
- Li, X., and M. A. Temerin (2001), The electron radiation belt, *Space Sci. Rev.*, *95*, 569.
- Li, X., et al. (1997), Multisatellite observations of the outer zone electron variation during the November 3–4, 1993, magnetic storm, *J. Geophys. Res.*, *102*, 14,123.
- Li, X., et al. (1999), Rapid enhancements of relativistic electrons deep in the magnetosphere during the May 15, 1997 magnetic storm, *J. Geophys. Res.*, *104*, 4467.
- Li, X., M. Temerin, D. N. Baker, G. D. Reeves, and D. Larson (2001), Quantitative prediction of radiation belt electrons at geostationary orbit based on solar wind measurements, *Geophys. Res. Lett.*, *28*, 1887.
- Li, L., J. Cao, and G. Zhou (2005a), Combined acceleration of electrons by whistler-mode and compressional ULF turbulences near the geosynchronous orbit, *J. Geophys. Res.*, *110*, A03203, doi:10.1029/2004JA010628.
- Li, X., D. N. Baker, M. Temerin, G. D. Reeves, R. Friedel, and C. Shen (2005b), Energetic electrons, 50 keV–6 MeV, at geosynchronous orbit: Their responses to solar wind variations, *Space Weather*, *3*, S04001, doi:10.1029/2004SW000105.
- Li, X., D. N. Baker, T. P. O'Brien, L. Xie, and Q. G. Zong (2006), Correlation between the inner edge of outer radiation belt electrons and the innermost plasmopause location, *Geophys. Res. Lett.*, *33*, L14107, doi:10.1029/2006GL026294.
- Li, W., Y. Y. Shprits, and R. M. Thorne (2007), Dynamic evolution of energetic outer zone electrons due to wave-particle interactions during storms, *J. Geophys. Res.*, *112*, A10220, doi:10.1029/2007JA012368.
- Liu, S., M. W. Chen, L. R. Lyons, H. Korth, J. M. Albert, J. L. Roeder, P. C. Anderson, and M. F. Thomsen (2003), Contribution of convective transport to stormtime ring current electron injection, *J. Geophys. Res.*, *108*(A10), 1372, doi:10.1029/2003JA010004.
- Loto'aniu, T. M., I. R. Mann, L. G. Ozeke, A. A. Chan, Z. C. Dent, and D. K. Milling (2006), Radial diffusion of relativistic electrons into the radiation belt slot region during the 2003 Halloween geomagnetic storms, *J. Geophys. Res.*, *111*, A04218, doi:10.1029/2005JA011355.
- Lyons, L. R., and R. M. Thorne (1972), Parasitic pitch angle diffusion of radiation belt particles by ion cyclotron waves, *J. Geophys. Res.*, *77*, 5608.
- Lyons, L. R., and D. J. Williams (1984), *Quantitative Aspects of Magnetospheric Physics*, Springer, New York.
- Lyons, L. R., R. M. Thorne, and C. F. Kennel (1972), Pitch-angle diffusion of radiation belt electrons within the plasmasphere, *J. Geophys. Res.*, *77*, 3455.
- Mathie, R. A., and I. R. Mann (2000), A correlation between extended intervals of ULF wave power and storm-time geosynchronous relativistic electron flux enhancements, *Geophys. Res. Lett.*, *27*, 3261.
- Meredith, N. P., R. B. Horne, and R. R. Anderson (2001), Substorm dependence of chorus amplitudes: Implications for the acceleration of electrons to relativistic energies, *J. Geophys. Res.*, *106*, 13,165.
- Meredith, N. P., R. B. Horne, R. H. A. Iles, R. M. Thorne, R. R. Anderson, and D. Heynderickx (2002a), Outer zone relativistic electron acceleration associated with substorm enhanced whistler mode chorus, *J. Geophys. Res.*, *107*(A7), 1144, doi:10.1029/2001JA001146.
- Meredith, N. P., R. B. Horne, D. Summers, R. M. T. R. H. A. Iles, D. Heynderickx, and R. R. Anderson (2002b), Evidence for acceleration of outer zone electrons to relativistic energies by whistler mode chorus, *Ann. Geophys.*, *20*, 967.
- Meredith, N. P., M. Cain, R. B. Horne, R. M. Thorne, D. Summers, and R. R. Anderson (2003a), Evidence for chorus driven electron acceleration to relativistic energies from a survey of geomagnetically disturbed periods, *J. Geophys. Res.*, *108*(A6), 1248, doi:10.1029/2002JA009764.
- Meredith, N. P., R. B. Horne, R. M. Thorne, and R. R. Anderson (2003b), Favored regions for chorus-driven electron acceleration to relativistic energies in the Earth's outer radiation belt, *Geophys. Res. Lett.*, *30*(16), 1871, doi:10.1029/2003GL017698.
- Meredith, N. P., R. B. Horne, S. A. Glauert, and R. R. Anderson (2007), Slot region electron loss timescales due to plasmaspheric hiss and lightning-generated whistlers, *J. Geophys. Res.*, *112*, A08214, doi:10.1029/2007JA012413.
- Parrot, M., and C. A. Gaye (1994), A statistical survey of ELF waves in a geostationary orbit, *Geophys. Res. Lett.*, *21*, 2463.
- Parrot, M., and F. Lefeuvre (1986), Statistical study of the propagation characteristics of ELF hiss observed on GEOS-1, inside and outside the plasmasphere, *Ann. Geophys.*, *4*, 363.
- Reeves, G. D., K. L. McAdams, R. H. W. Friedel, and T. P. O'Brien (2003), Acceleration and loss of relativistic electrons during geomagnetic storms, *Geophys. Res. Lett.*, *30*(10), 1529, doi:10.1029/2002GL016513.
- Reeves, G. D., et al. (1998), The relativistic electron response at geosynchronous orbit during the January 1997 magnetic storm, *J. Geophys. Res.*, *103*, 17,559.
- Roth, I., M. Temerin, and M. K. Hudson (1999), Resonant enhancement of relativistic electron fluxes during geomagnetically active periods, *Ann. Geophys.*, *17*, 631.
- Santolík, O., D. A. Gurnett, J. S. Pickett, M. Parrot, and N. Cornilleau-Wehrin (2003), Spatio-temporal structure of storm-time chorus, *J. Geophys. Res.*, *108*(A7), 1278, doi:10.1029/2002JA009791.
- Santolík, O., D. A. Gurnett, J. S. Pickett, M. Parrot, and N. Cornilleau-Wehrin (2004), A microscopic and nanoscopic view of storm-time chorus on 31 March 2001, *Geophys. Res. Lett.*, *31*, L02801, doi:10.1029/2003GL018757.
- Sarris, T., X. Li, and M. Temerin (2006), Simulating radial diffusion of energetic (MeV) electrons through a model of fluctuating electric and magnetic fields, *Ann. Geophys.*, *24*, 1.
- Schulz, M., and L. J. Lanzerotti (1974), *Particle Diffusion in the Radiation Belts*, *Phys. Chem. Space*, vol. 7, Springer-Verlag, New York.
- Selesnick, R. S., and J. B. Blake (2002), Relativistic electron drift shell splitting, *J. Geophys. Res.*, *107*(A9), 1265, doi:10.1029/2001JA009179.
- Sheeley, B. W., M. B. Moldwin, H. K. Rassoul, and R. R. Anderson (2001), An empirical plasmasphere and trough density model: CRRES observations, *J. Geophys. Res.*, *106*, 25,631.
- Shprits, Y. Y., and R. M. Thorne (2004), Time dependent radial diffusion modeling of relativistic electrons with realistic loss rates, *Geophys. Res. Lett.*, *31*, L08805, doi:10.1029/2004GL019591.
- Shprits, Y. Y., R. M. Thorne, G. D. Reeves, and R. Friedel (2005), Radial diffusion modeling with empirical lifetimes: Comparison with CRRES observations, *Ann. Geophys.*, *23*, 1467.

- Shprits, Y. Y., R. M. Thorne, R. B. Horne, M. Cartwright, C. T. Russell, D. Baker, and S. G. Kanekal (2006a), Acceleration mechanism responsible for the formation of the new radiation belt during the 2003 Halloween solar storm, *Geophys. Res. Lett.*, *33*, L05104, doi:10.1029/2005GL024256.
- Shprits, Y. Y., R. M. Thorne, R. B. Horne, and D. Summers (2006b), Bounce-averaged diffusion coefficients for field-aligned chorus waves, *J. Geophys. Res.*, *111*, A10225, doi:10.1029/2006JA011725.
- Skoug, R. M., S. Datta, M. P. McCarthy, and G. K. Parks (1996), A cyclotron resonance model of VLF chorus emissions detected during electron microburst precipitation, *J. Geophys. Res.*, *101*, 21,481.
- Smith, A. J., R. M. Thorne, and M. P. Meredith (2004), Ground observations of chorus following geomagnetic storms, *J. Geophys. Res.*, *109*, A02205, doi:10.1029/2003JA010204.
- Smith, E. J., A. M. A. Frandsen, B. T. Tsurutani, R. M. Thorne, and K. W. Chan (1974), Plasmaspheric hiss intensity variations during magnetic storms, *J. Geophys. Res.*, *79*, 2507.
- Steinacker, J., and J. A. Miller (1992), Stochastic gyroresonant electron acceleration in a low-beta plasma, I. Interaction with parallel transverse cold plasma waves, *Astrophys. J.*, *393*, 764.
- Stix, T. H. (1992), *Waves in Plasmas*, American Institute of Physics, New York.
- Summers, D. (2005), Quasi-linear diffusion coefficients for field-aligned electromagnetic waves with applications to the magnetosphere, *J. Geophys. Res.*, *110*, A08213, doi:10.1029/2005JA011159.
- Summers, D., and C. Ma (2000), A model for generating relativistic electrons in the Earth's inner magnetosphere based on gyroresonant wave-particle interactions, *J. Geophys. Res.*, *105*, 2625.
- Summers, D., and R. M. Thorne (2003), Relativistic electron pitch-angle scattering by electromagnetic ion cyclotron waves during geomagnetic storms, *J. Geophys. Res.*, *108*(A4), 1143, doi:10.1029/2002JA009489.
- Summers, D., R. M. Thorne, and F. Xiao (1998), Relativistic theory of wave-particle resonant diffusion with application to electron acceleration in the magnetosphere, *J. Geophys. Res.*, *103*, 20,487.
- Summers, D., C. Ma, N. P. Meredith, R. B. Horne, R. M. Thorne, D. Heynderickx, and R. R. Anderson (2002), Model of the energization of outer-zone electrons by whistler mode chorus during the October 9, 1990 geomagnetic storm, *Geophys. Res. Lett.*, *29*(24), 2174, doi:10.1029/2002GL016039.
- Summers, D., C. Ma, N. P. Meredith, R. B. Horne, R. M. Thorne, and R. R. Anderson (2004), Modeling outer-zone relativistic electron response to whistler mode chorus activity during substorms, *J. Atmos. Sol. Terr. Phys.*, *66*, 133.
- Summers, D., B. Ni, and N. P. Meredith (2007a), Timescales for radiation belt electron acceleration and loss due to resonant wave-particle interactions: 1. Theory, *J. Geophys. Res.*, *112*, A04206, doi:10.1029/2006JA011801.
- Summers, D., B. Ni, and N. P. Meredith (2007b), Timescales for radiation belt electron acceleration and loss due to resonant wave-particle interactions: 2. Evaluation for VLF chorus, ELF hiss, and electromagnetic ion cyclotron waves, *J. Geophys. Res.*, *112*, A04207, doi:10.1029/2006JA011993.
- Thorne, R. M. (1977), Energetic radiation belt electron precipitation: A natural depletion mechanism for stratospheric ozone, *Science*, *195*, 287.
- Thorne, R. M., and R. B. Horne (1996), Whistler absorption and electron heating near the plasmapause, *J. Geophys. Res.*, *101*, 4917.
- Thorne, R. M., E. J. Smith, K. J. Fiske, and S. R. Church (1974), Intensity variation of elf hiss and chorus during isolated substorms, *Geophys. Res. Lett.*, *1*, 193.
- Thorne, R. M., R. B. Horne, S. A. Glauert, N. P. Meredith, Y. Shprits, D. Summers, and R. R. Anderson (2005), The influence of wave-particle interactions on relativistic electron dynamics during storms, in *Inner Magnetosphere Interactions: New Perspectives From Imaging*, *Geophys. Monogr. Ser.*, vol. 159, edited by J. Burch, M. Schulz, and H. Spence, p. 101, AGU, Washington, D. C.
- Thorne, R. M., Y. Y. Shprits, N. P. Meredith, R. B. Horne, W. Li, and L. R. Lyons (2007), Refilling of the slot region between the inner and outer electron radiation belts during geomagnetic storms, *J. Geophys. Res.*, *112*, A06203, doi:10.1029/2006JA012176.
- Tsurutani, B. T., and E. J. Smith (1974), Postmidnight chorus: A substorm phenomenon, *J. Geophys. Res.*, *79*, 118.
- Tsurutani, B. T., and E. J. Smith (1977), Two types of magnetospheric ELF chorus and their substorm dependences, *J. Geophys. Res.*, *82*, 5112.
- Tsurutani, B. T., E. J. Smith, and R. M. Thorne (1975), Electromagnetic hiss and relativistic electron losses in the inner zone, *J. Geophys. Res.*, *80*, 600.
- Varotsou, A., D. Boscher, S. Bourdarie, R. B. Horne, S. A. Glauert, and N. P. Meredith (2005), Simulation of the outer radiation belt electrons near geosynchronous orbit including both radial diffusion and resonant interaction with whistler-mode chorus waves, *Geophys. Res. Lett.*, *32*, L19106, doi:10.1029/2005GL023282.
- Walt, M., H. D. Voss, and J. Pickett (2002), Electron precipitation coincident with ELF/VLF wave bursts, *J. Geophys. Res.*, *107*(A8), 1208, doi:10.1029/2001JA009100.
- Xiao, F., R. M. Thorne, and D. Summers (1998), Instability of electromagnetic R-mode waves in a relativistic plasma, *Phys. Plasmas*, *5*, 2489.
- Xiao, F., H. Y. He, Q. H. Zhou, H. N. Zheng, and S. Wang (2006a), Relativistic diffusion coefficients for superluminescent (auroral kilometric radiation) wave modes in space plasmas, *J. Geophys. Res.*, *111*, A11201, doi:10.1029/2006JA011865.
- Xiao, F., Q. H. Zhou, H. N. Zheng, and S. Wang (2006b), Whistler instability threshold condition of energetic electrons by kappa distribution in space plasmas, *J. Geophys. Res.*, *111*, A08208, doi:10.1029/2006JA011612.
- Xiao, F., Q. H. Zhou, H. Y. He, and L. J. Tang (2006c), Instability of whistler-mode waves by a relativistic kappa-loss-cone distribution in space plasmas, *Plasma Phys. Controlled Fusion*, *48*, 1437.
- Xiao, F., R. M. Thorne, and D. Summers (2007a), Higher-order gyroresonant acceleration of electrons by superluminescent (AKR) wave-modes, *Planet. Space Sci.*, *55*, 1257.
- Xiao, F., Q. H. Zhou, H. Y. He, H. N. Zheng, and S. Wang (2007b), Electromagnetic ion cyclotron waves instability threshold condition of suprathermal protons by kappa distribution, *J. Geophys. Res.*, *112*, A07219, doi:10.1029/2006JA012050.
- Xiao, F., C. Shen, Y. Wang, H. Zheng, and S. Wang (2008), Energetic electron distributions fitted with a relativistic kappa-type function at geosynchronous orbit, *J. Geophys. Res.*, *113*, A05203, doi:10.1029/2007JA012903.
- Zong, Q.-G., et al. (2007), Ultralow frequency modulation of energetic particles in the dayside magnetosphere, *Geophys. Res. Lett.*, *34*, L12105, doi:10.1029/2007GL029915.

L. Chen and F. Xiao, School of Physics and Electronic Sciences, Changsha University of Science and Technology, Changsha, Hunan 410076, China. (chenliang_xu@126.com; flxiao@126.com)

Q.-G. Zong, School of Earth and Space Sciences, Peking University, Beijing 100871, China. (qgzong@pku.edu.cn)